

tions.

¹²R. K. Nesbet, Phys. Rev. **175**, 2 (1968).

¹³R. S. Berry and J. C. Mackie, J. Chem. Phys. **43**, 3067 (1965). The spin-orbit-coupling correction is negligible for $O(^3P_2)-O(^2P_{1/2})$.

¹⁴L. M. Branscomb, D. S. Burch, S. J. Smith, and S. Geltman, Phys. Rev. **111**, 504 (1958).

¹⁵C. M. Moser and R. K. Nesbet, Phys. Rev. A **4**, 1336 (1971).

PHYSICAL REVIEW A

VOLUME 5, NUMBER 6

JUNE 1972

L X-Ray Transition Probabilities in Elements of Medium and High Atomic Numbers

S. I. Salem, D. C. Clark, and R. T. Tsutsui

Department of Physics and Astronomy, California State University, Long Beach, California 90801

(Received 11 February 1972)

The $L\gamma_2/L\beta_3$, $L\gamma_3/L\beta_3$, $L\eta/L\beta_1$, $L\beta_5/L\alpha_1$, $L\beta_6/L\alpha_1$, and $Ll/L\alpha_1$ radiative-transition probability ratios have been measured for 13 elements ranging in atomic number from ${}_{62}\text{Sm}$ to ${}_{92}\text{U}$. This has been accomplished by bombarding the elements with an electron beam of constant energy and flux, and counting the x-ray photons emitted by a given electronic transition. The corrected measured ratios are compared with the results calculated on the basis of the relativistic-Hartree-Fock-Slater (RHFS) potential and those calculated on the basis of the relativistic-screened-Coulomb (RSC) potential. In general, values calculated on the basis of RHFS potential are favored except for the $Ll/L\alpha_1$ ratio where the measured values and those obtained from a RSC-potential calculations are in excellent agreement and are as much as 40% lower than the values obtained assuming a RHFS potential. The $L\gamma_2/L\beta_3$ and $L\gamma_3/L\beta_3$ values obtained with a RSC potential are as much as an order of magnitude greater than experimental values at high Z , and are not included in the graphs. The estimated error of the experimental results is from 10 to 15%. Other experimental values are also included for comparison.

INTRODUCTION

The $L\beta_3/L\beta_4$, $L\gamma_1/L\beta_1$, $L\alpha_2/L\alpha_1$, $L\beta_{2,15}/L\alpha_1$, and $L\beta_{2,15}/L\alpha_2$ radiative-transition probability ratios have recently been measured for a large number of elements ranging in atomic number from lanthanum to uranium.¹ Work has been extended to cover the less prominent transitions in the same range of atomic number. Previous work on these less prominent L x-ray transitions,²⁻¹² has never been carried out for the rare-earth elements, and their recently tabulated values are mere extrapolations.¹³

Recent relativistic calculations of L x-ray transition probabilities were carried out by Babushkin,¹⁴ Scofield,¹⁵ and by Rosner and Bhalla.¹⁶ Scofield and Rosner and Bhalla assumed that the electron states are in a self-consistent central field derived from a relativistic-Hartree-Fock-Slater (RHFS) potential¹⁷:

$$V(r) = -\frac{Ze^2}{r} + \frac{e^2}{r} \int_0^r 4\pi r'^2 \rho(r') dr' + e^2 \int_r^\infty 4\pi r' \rho(r') dr' - e^2 [(81/8\pi)\rho(r)]^{1/3}. \quad (1)$$

Babushkin carried out his calculations for electrons in a relativistic-screened-Coulomb (RSC) potential; he made use of Dirac wave functions screened by

Burns's prescription.¹⁸ Babushkin's numerical results are given as intensity ratios rather than relative transition probabilities and for comparison were transformed to transition probabilities by the relation

$$P_i = I_i / \hbar \omega_i, \quad (2)$$

where the subscript i indicates a transition of energy $\hbar \omega_i$.

A retarded radiation field was assumed in all the

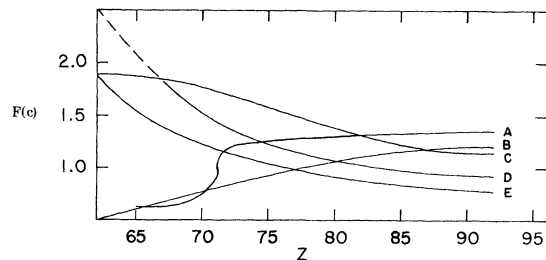


FIG. 1. Calculated correction factors $F(c)$ applied to the transition probability ratios plotted as a function of atomic number. Corrections account for differential absorption, reflectivity of the crystal, and the efficiency of the detector. We have the following: $A = L\beta_5/L\alpha_1$, $B = L\beta_6/L\alpha_1$, $C = L\gamma_2/L\beta_3 = L\gamma_1/L\beta_3$, $D = Ll/L\alpha_1$, and $E = L\eta/L\beta_1$.

TABLE I. Measured corrected radiative-transition-probability ratios.

| Element | $(L\gamma_2/L\beta_3)100$ | $(L\gamma_3/L\beta_3)100$ | $(L\eta/L\beta_1)100$ | $(L\beta_5/L\alpha_1)100$ | $(L\beta_6/L\alpha_1)100$ | $(Ll/L\alpha_1)100$ |
|------------------|---------------------------|---------------------------|-----------------------|---------------------------|---------------------------|---------------------|
| ^{62}Sm | | | | | 0.66 | 2.39 |
| ^{65}Tb | 16.5 | 22.3 | | | | 2.64 |
| ^{67}Ho | 16.0 | 32.4 | | | 0.57 | 2.82 |
| ^{69}Tm | 21.5 | 29.2 | 1.95 | | 1.08 | 3.11 |
| ^{71}Lu | 25.3 | 30.8 | 1.36 | 0.39 | | 3.48 |
| ^{72}Hf | 27.2 | 33.2 | 1.57 | 0.69 | | 3.06 |
| ^{73}Ta | 25.7 | | 1.79 | | | 3.79 |
| ^{74}W | 19.6 | 26.0 | 1.60 | 0.72 | 1.27 | 3.38 |
| ^{77}Ir | 18.7 | 20.6 | 1.49 | 1.02 | | 4.81 |
| ^{79}Au | 26.6 | 27.2 | 2.40 | 2.20 ^a | 1.20 ^a | 3.96 |
| ^{83}Bi | 25.2 | 40.0 | 2.14 | 3.11 | 2.00 ^a | 4.83 |
| ^{90}Th | 35.8 | 48.6 | 2.81 | | 1.69 | 5.19 |
| ^{92}U | 41.7 | 45.0 | 3.45 | 5.90 ^a | 1.73 | 4.93 |

^aFrom Ref. 1.

above calculations. The effect of the finite size of the nucleus on such calculations amounts to only a fraction of 1% for some of the K transitions and is of significantly smaller magnitude when evaluated in connection with L transitions. Of the recent calculations only Rosner and Bhalla included such an effect. The numerical results obtained by Rosner and Bhalla agree with those obtained by Scofield to within three significant figures and are indistinguishable in the scales at which the graphs in this paper are drawn.

EXPERIMENTAL

The elements studied were all in solid forms and varied in purity from 99.99% for gold and tungsten to 99.9% for the rare-earth elements. Except for ^{83}Bi , all the elements were in the form of foils varying in thickness from 0.5 to 0.13 mm. Backing was provided for all the foils before being fitted into the water-cooled-anode assembly. Bismuth ingots were melted in a copper container, and its surface was smoothed and cleaned before being introduced into the vacuum chamber. The foils of the

rare-earth elements and those of ^{90}Th and ^{92}U were placed at the surface of a copper dish filled with ^{31}Ga . The copper dish was water cooled for the duration of the experiment. The molten gallium in this arrangement proved to be satisfactory in keeping the thin foils from evaporating under electron bombardment.

The electron beam used in ionizing the target atoms was provided by a tungsten filament 0.127 mm in diameter and about 2 cm long, fitted in a stainless-steel focusing cup. The filament is heated by means of an insulated transformer, as the filament assembly was maintained at a negative high potential. The electron energy was provided by a power supply connected in series with a line-voltage regulator and a ripple suppressor. This system is capable of delivering a steady voltage with less than 0.3% ripple at a full load of 120 keV and 30 mA. The energy of the electron beam was maintained at 25 ± 0.1 keV when elements with $Z \leq 83$ were under investigation and at 40 ± 0.1 keV during the study of thorium and uranium. The electron current output was maintained at 0.50 ± 0.01

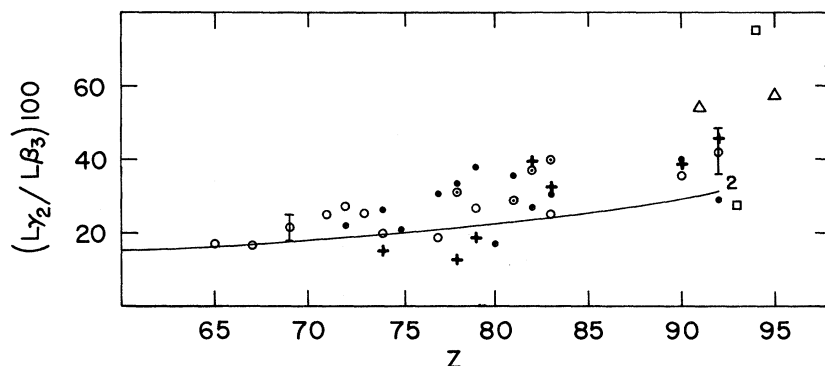


FIG. 2. $L\gamma_2/L\beta_3$ transition-probability ratio plotted as a function of atomic number Z . Curve 2 is from Ref. 15. The experimental points are \bullet (Ref. 8), $+$ (Ref. 7), \square (Ref. 10), Δ (Ref. 11), \circ (Ref. 1), and \circ (present work).

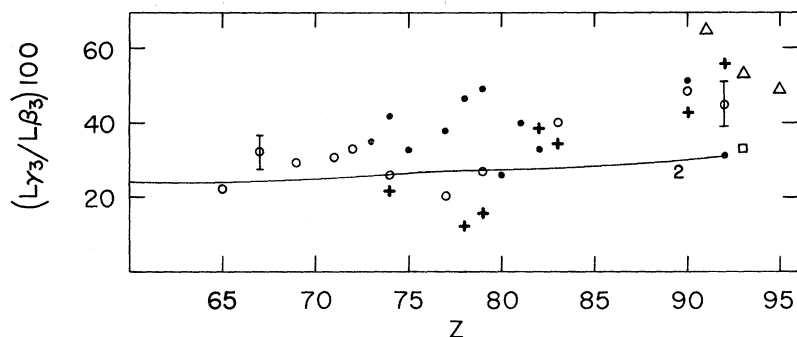


FIG. 3. $L\gamma_3/L\beta_3$ transition-probability ratio plotted as function of atomic numbers Z . The curve label and the symbols have the same designation as in Fig. 2.

mA throughout the experiment.

A modified high-angle single-crystal goniometer was used to scan over the region of interest, and for each sample, the studied transitions were measured in steps of 0.005° in the Bragg angle 2θ . At each position, the number of counts were recorded for a period of 60 sec. At least four runs for each transition were taken and averaged.

Rather than comparing peak intensities as one normally does where the widths of the characteristic lines are very nearly the same, here the areas under these curves were considered proportional to the transition probabilities because the width of the measured lines did not appear to be all the same. For example, the widths of the $L\ell$ lines are significantly larger than those of the $L\alpha_1$ lines.

In elements where two characteristic lines were not far enough apart to be mutually free from contributions arising from the Lorentzian tails associated with x-ray characteristic lines, or were not completely resolved as is the case with $L\gamma_2$ and $L\gamma_3$ lines in elements with $Z \leq 74$, the two lines were unfolded and the overlapping portions were measured and their undesired contributions eliminated.

One of the difficulties in measuring weak and medium transitions in the L spectrum of medium- and high-atomic-number elements is the presence of extremely strong lines that could completely

overshadow these weak ones when they happen to be close together as is the case with $L\eta$ and $L\alpha_1$ in ${}_{62}\text{Sm}$ and ${}_{65}\text{Tb}$. Another difficulty is the presence of very weak transitions whose values have never been measured or calculated, and whose contributions when they happen to be in the proximity of a medium transition is hard to estimate. Thus, the value reported for $L\beta_5$ in ${}_{75}\text{Re}$ is probably high because of contributions from $L\beta_{10}$ and $L\beta_7$. Similarly the value reported in Ref. 1 for $L\beta_5$ of uranium is probably in error because of contributions from $L_{\text{III}} - P_{\text{I}}$ and $L_{\text{III}} - P_{\text{IV,V}}$ transitions. Still another problem arises when one of the L -absorption edges falls too close to one of the emission lines under study, which is the situation of the L_{III} - absorption edge and the $L\beta_5$ transition in ${}_{73}\text{Ta}$. For the elements ${}_{71}\text{Lu}$, ${}_{72}\text{Hf}$, and ${}_{73}\text{Ta}$ the most probable values of $L\beta_6$, from Fig. 6, had to be subtracted from $L\beta_1$ in order to obtain a value of the ratio $L\eta/L\beta_1$ for these elements. To obtain the values of $L\gamma_2/L\beta_3$ and $L\gamma_3/L\beta_3$ for gold, measurements were made for the $L\gamma_2/L\beta_4$ and $L\gamma_3/L\beta_4$ from which, with the help of the most probable value of $L\beta_3/L\beta_4$ from Ref. 1, the desired ratios were calculated. All these steps, which cannot be avoided under the present experimental conditions, introduce additional errors.

To reduce the effect of self-absorption in the anode material, a process complicated by photo-

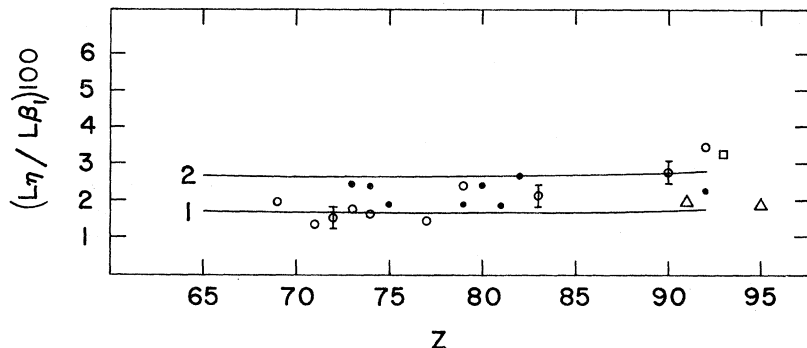


FIG. 4. $L\eta/L\beta_1$ transition-probability ratio plotted as a function of atomic number Z . Curve 1 is from Ref. 14, and curve 2 is from Ref. 15, and the symbols have the same designation as in Fig. 2.

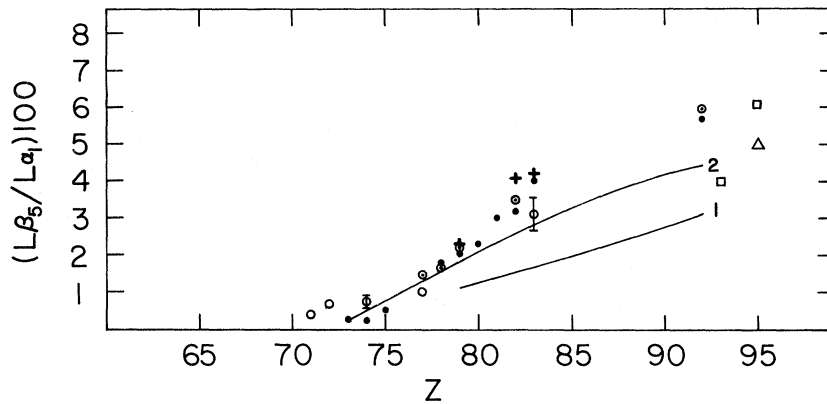


FIG. 5. $L\beta_5/L\alpha_1$ transition-probability ratio plotted as a function of atomic number. The curves numbers and the symbols have the same designation as in the previous figures.

ionization,¹⁹ the energy of the electron beam was kept at a practical low value and the take-off angle was set at 15° . The mean depth of formation of x-ray characteristic lines was calculated from previously measured values²⁰ and the fact that such depth is inversely proportional to the electron density of the material traversed. Further corrections were made for the counter recovery time, for differential self-absorption, for absorption in the ${}^4\text{Be}$ x-ray-tube window and in the air path, for the reflectivity R_c of the calcite crystal, and for the efficiency E_c of the ${}_{54}\text{Xe}$ -filled Geiger-Müller counter as a function of the photon energy. The correction factor is

$$F(c) = (R_c F_c)^{-1} \exp + (\sum_j \mu_j \rho_j t_j) \exp(\mu_t \rho_t t_t \csc \Psi), \quad (3)$$

where μ_j , ρ_j , and t_j are, respectively, the mass absorption coefficients, the mass densities, and the thicknesses of the material traversed by the photons before reaching the counter. Here μ_t is the mass-absorption coefficient of the target material for its own characteristic lines. ρ_t is the target mass density, t_t is the depth of formation of characteristic lines, and Ψ is the take-off angle. The values of the mass-absorption coefficients were obtained from the tables of McMaster *et al.*²¹ Equation (3) was computer solved for all the reported transition-probability ratios of the elements studied. The values of the correction factor for the indicated ratios are shown in Fig. 1. The correction factors for $L\gamma_2/L\beta_3$ and for $L\gamma_3/L\beta_3$ are

nearly the same for all the elements except ${}_{79}\text{Au}$, where the L_{II} -absorption edge lies between $L\gamma_2$ and $L\gamma_3$. Only one correction curve is shown for these two ratios.

Several sources contribute to errors in the experimental results. The most important ones are (a) counting statistics, (b) systematic errors, (c) voltage and current instabilities, (d) tungsten and carbon contamination of the sample under study, (e) spectrum unfolding, (f) difficulties in evaluating the background radiation because of the complex nature of the L spectrum, and (g) errors in evaluating $F(c)$. To reduce statistical errors, the spectrum of each element was measured several times, and the average values are reported. Systematic errors were also reduced by alternating the stepping directions of the Bragg angle for successive runs. An average value of $F(c)$ was used by drawing smooth curves through the calculated values. An error analysis was carried out for all the measured ratios. These were found to be between 10 and 15% for all the measured quantities, and their magnitudes are indicated by error bars in the appropriate graphs.

RESULTS AND DISCUSSION

The corrected numerical results of this work are presented in Table I, as transition-probability ratios. This table also includes ratios previously reported in Ref. 1. Transitions originating at each of the three L subshells are reported as fractions of the most prominent transition to that particular sub-

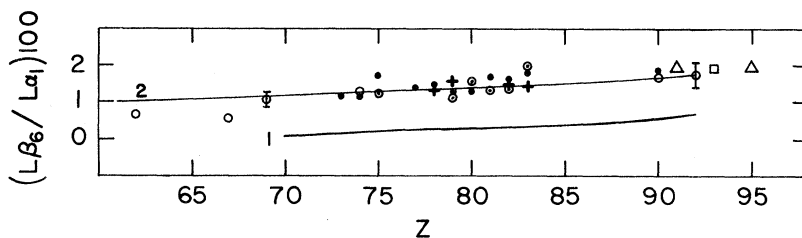


FIG. 6. $L\beta_6/L\alpha_1$ transition-probability ratio plotted as a function of atomic number Z . The curves numbers and symbols have the same designation as in the previous figures.

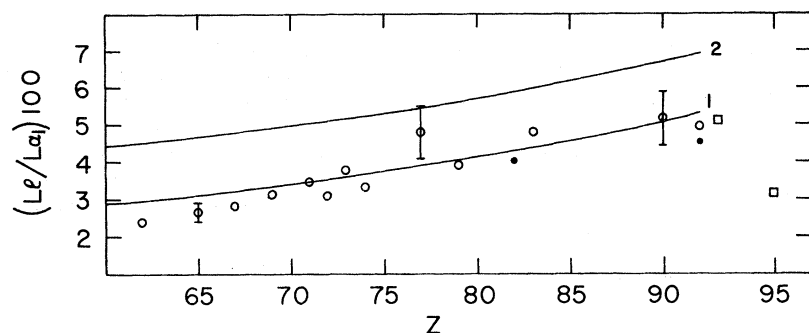


FIG. 7. $Ll/L\alpha_1$ transition-probability ratio plotted as a function of atomic number Z . The curves' numbers and symbols have the same designation as in the previous figures.

shell. Thus, for example, the values of $L\beta_5$, $L\beta_6$, and Ll are given relative to $L\alpha_1$. Normalizing all the L transition probabilities relative to that of $L\alpha_1$ ²² is physically insignificant.

Measurements were not performed for elements with atomic numbers lower than 62, as some of these transitions became too weak for accurate measurements as Z approaches this value. The correction factor $F(c)$ Fig. 1, increases rapidly for most transitions as the atomic number decreases. Furthermore, it became rather difficult to resolve the $L\gamma_2$ and the $L\gamma_3$ lines, and practically impossible to observe $L\eta$.

Figures 2-7 are plots of the indicated measured transition probabilities as functions of the atomic numbers of the studied elements. Also plotted are the experimental values from Ref. 1, 7, 8, 10, and 11, and Scofield's and Babushkin's theoretical values. The values of $L\gamma_2/L\beta_3$ and $L\gamma_3/L\beta_3$ reported by Babushkin were extremely high and are not included. Except for a few values from Ref. 10, all the experimental results are in agreement within reported errors. The results of this work seem to agree reasonably well with the theoretical results obtained on the basis of a RHFS potential for the ratios $L\gamma_2/L\beta_3$ (Fig. 2), $L\beta_5/L\alpha_1$ (Fig. 5), and $L\beta_6/L\alpha_1$ (Fig. 6). The experimental values are generally higher than the theoretical results for the $L\gamma_3/L\beta_3$ transition-probability ratio, Fig. 3. This varies from some 15% at about $Z = 70$ to as much as 30% for higher atomic numbers. Figure 4 shows that the experimental values of $L\eta/L\beta_1$

generally fall between the two theoretical values with a tendency to rise with atomic number at a rate faster than either theory indicates. Figure 7 shows that the results of this experiment for the $Ll/L\alpha_1$ transition-probability ratio are in excellent agreement with the theoretical values obtained assuming a RSC potential. In turn, this is in very good agreement with the experimental results of Ref. 2, 4, 8, and 10. Allison's data³ for ${}_{90}\text{Th}$ and ${}_{92}\text{U}$ is considerably lower. The results obtained by Rao *et al.*⁹ fall almost midway between the two theoretical values, and the recent results of McCrary *et al.*¹² are considerably higher; these values were reported as being higher than the theoretical results of Scofield.

CONCLUSION

The present experimental results indicate that the theoretical results based on a RHFS potential are generally favored. But exceptions to this general agreement are becoming numerous, and the magnitude of the discrepancies seems to increase as the energy difference between compared transitions increases.²³

The excellent agreement between experimental results and the results based on RSC potential in the case of $Ll/L\alpha_1$ ratio needs to be mentioned and probably emphasized, as it is not an isolated case. The results based on RSC potential seem to approach good agreement with experimental values, when the energy difference between compared transitions is relatively large.

¹S. I. Salem, R. T. Tsutsui, and B. A. Rabbani, Phys. Rev. A **4**, 1728 (1971).

²A. Jonsson, Z. Physik **36**, 426 (1926).

³S. K. Allison, Phys. Rev. **30**, 245 (1927); **38**, 572 (1931).

⁴V. Hicks, Phys. Rev. **36**, 1273 (1930); **38**, 572 (1931).

⁵V. J. Andrew, Phys. Rev. **42**, 591 (1932).

⁶R. W. G. Wyckoff and F. D. Davidson, Phys. Rev. **36**, 1883 (1965).

⁷C. Victor, Ann. Phys. (Paris) **6**, 183 (1961).

⁸M. Goldberg, Ann. Phys. (Paris) **7**, 329 (1962).

⁹V. Rao, J. M. Palms, and R. E. Wood, Phys. Rev. A **3**, 1568 (1971).

¹⁰P. P. Day, Phys. Rev. **97**, 689 (1955).

¹¹H. Jaffe, T. O. Passell, C. I. Brown, and I. Perlman, Phys. Rev. **97**, 142 (1955).

¹²J. H. McCrary, L. V. Singman, L. H. Ziegler, L. D. Looney, C. M. Edmonds, and C. E. Harris, Phys. Rev. A **5**, 1587 (1972).

¹³S. I. Salem and C. W. Schultz, At. Data (to be published).

¹⁴F. A. Babushkin, Acta Phys. Polon. **35**, 883 (1969).

- ¹⁵J. H. Scofield, *Phys. Rev.* **179**, 9 (1969).
¹⁶H. R. Rosner and C. P. Bhalla, *Z. Physik* **231**, 347 (1970).
¹⁷D. Liberman, J. T. Waber, and D. T. Cramer, *Phys. Rev. A* **142**, 604 (1970).
¹⁸G. Burns, *J. Chem. Phys.* **41**, 1521 (1964).
¹⁹S. I. Salem and D. G. Zarlingo, *Phys. Rev.* **155**, 7 (1967).
²⁰S. I. Salem and J. C. Watts, *J. Chem. Phys.* **39**, 2259 (1963).
²¹W. H. McMaster, N. Kerr Del Grande, J. H. Mallet, and J. H. Hubbel, Lawrence Radiation Laboratory Report No. UCRL-50174, 1967, Sec. 11, Rev. 1 (unpublished).
²²A. H. Compton and S. K. Allison, *X-Rays in Theory and Experiment* (Van Nostrand, New York, 1935), p. 642.
²³P. J. Ebert and V. W. Slivinsky, *Phys. Rev.* **188**, 1 (1969); G. C. Nelson, B. G. Saunders, and S. I. Salem, *At. Data* **1**, 377 (1970).

PHYSICAL REVIEW A

VOLUME 5, NUMBER 6

JUNE 1972

Configuration-Space Hamiltonian for Heavy Atoms and Correction to the Breit Interaction*

Marvin H. Mittleman

The City College of the City University of New York, New York, New York 10031

(Received 21 September 1971)

The lowest-order configuration-space Hamiltonian (CSH) for a heavy atom is constructed from quantum electrodynamics by a variational procedure. A variational potential function Ω is introduced which in effect allows some freedom in the choice of the definition of the difference between electrons and positrons. The optimization of Ω results in a nonlinear equation from which it is shown that Ω is probably not small for relativistic electrons. The procedure results in a CSH which contains a new two-body interaction which is relativistic in origin and which is apparently of the same order of magnitude as the Breit interaction when acting between relativistic electrons.

I. INTRODUCTION

In the first paper of this series (I)¹ the problem of the extraction of a configuration-space Hamiltonian (CSH) for a heavy atom from the usual quantum-electrodynamic (QED) formulation of the problem was discussed. A review of the existing situation was presented. The fact that the most obvious generalization of the Schrödinger CSH, a sum of single-particle Dirac Hamiltonians with simple two-body interactions, leads to difficulties² (Brown's disease) was reviewed. The three-electron potential interactions were derived for the situation where there are only a few electrons (i. e., where $N\alpha \ll 1$, here N is the number of electrons). The assumption was then made that the derived form applies even when there are many electrons and that the total energy residing in the three-body potential would then be the sum of this form over all different triplets of electrons in the atom. In that case it was possible to show that the total three-body energy is of the order of a few rydbergs, a small part of the total energy of the atom.

We now return to the problem of the CSH of a heavy atom retaining only lowest-order terms. For example, we shall find the leading two-body potential will be of order e^2 but there will be corrections to the two-body interaction of order e^4 and smaller. These will be neglected. For this rea-

son we shall never encounter renormalization problems here. However, extension of this work will run into these problems and it is not obvious how they will best be handled. We shall also neglect three-body potentials because of the author's previous work.¹ This is not completely justified since the three-body results described in I depend on the form of the two-body potential and this form changes in the many electron system considered here from the form for the few electron system in I. Thus our neglect of the three-body potentials here is not rigorous and will have to be reinvestigated subsequently.

A method for obtaining a CSH would be to expand the Fock-space wave function in an infinite series of terms. The first has N electrons, the second $N+1$ electrons and one positron, and each additional term has an extra pair. The amplitude function of the first term may then be considered the wave function of the atom. We can then obtain an infinite set of equations coupling all the amplitude functions. We could eliminate all but the first, thereby obtaining the required Hamiltonian but this procedure would result in an intractable operator (if it exists at all). We take the point of view here that the elimination of even one other function would complicate the resulting CHS beyond the point of usefulness. Therefore we seek an expression for the Fock-space wave function which contains only